

Experimental Determination Of The Pull-Out Strength Of Cast-In Lifting Inserts In Precast Hollow-Core Plank

Salvador Murra
Marquette University

Recommended Citation

Murra, Salvador, "Experimental Determination Of The Pull-Out Strength Of Cast-In Lifting Inserts In Precast Hollow-Core Plank" (2013). *Master's Theses (2009 -)*. Paper 195.
http://epublications.marquette.edu/theses_open/195

EXPERIMENTAL DETERMINATION OF THE PULL-OUT STRENGTH
OF CAST-IN LIFTING INSERTS IN PRECAST
HOLLOW-CORE PLANK

by

Salvador Murra

A Thesis submitted to the Faculty of the Graduate School,
Marquette University,
In Partial Fulfillment of the Requirements for
The Degree of Master of Science

Milwaukee, Wisconsin

May 2013

ABSTRACT
EXPERIMENTAL DETERMINATION OF THE PULL OUT STRENGTH
OF CAST-IN LIFTING INSERTS IN PRECAST
HOLLOW-CORE PLANK

Salvador Murra

Marquette University, 2013

Hollow-Core precast plank is a commonly used building component. The common method to lift and erect these planks is through the use of slings. This method has several drawbacks and has spurred on the current effort to investigate and determine the capacity of lifting inserts post-installed into the top of precast hollow-core planks. The insert that was studied is the P-52 “Swift Lift” Insert supplied by Dayton-Superior.

Physical testing of 16 inserts was done to aid in determining the tensile capacity of the insert. The insert was a 3/4" diameter steel insert by 5 1/2" long and it was post installed using non-shrink grout into the top of a hollowcore plank shortly after it was extruded. A literature review was also performed to further analyze the insert and to formulate analytical expressions capable of reliably predicting this tensile (pull-out) capacity of the insert.

The testing resulted in an average measured tensile capacity of 13.8 kips with a standard deviation of 1.85 kips. Our predictive model gave us a capacity of 12.33 kips which is within one standard deviation from the average measured capacity. A factor of safety of 2.2 was also calculated and developed. When we apply our factor of safety to our measured tensile capacity we obtain a recommended capacity of 6.2 kips.

TABLE OF CONTENTS

| | |
|---|----|
| ABSTRACT..... | i |
| TABLE OF CONTENTS..... | ii |
| CHAPTERS | |
| I. INTRODUCTION..... | 1 |
| II. LITERATURE REVIEW & SYNTHESIS..... | 6 |
| III. EXPERIMENTAL TESTING..... | 21 |
| IV. EXPERIMENTAL RESULTS & DISCUSSION..... | 34 |
| V. CONCLUSIONS & RECOMMENDATIONS FOR FUTURE WORK..... | 49 |
| BIBLIOGRAPHY..... | 53 |
| APPENDIX | |
| A. SPANCRETE PLANK DESIGN TABLE..... | 54 |
| B. DAYTON-SUPERIOR PRODUCT HANDBOOK [PAGE 26]..... | 55 |
| C. DAYTON-SUPERIOR PRODUCT HANDBOOK [PAGE 28]..... | 56 |

CHAPTER 1

INTRODUCTION

1.1 Background Information

Hollow-Core precast plank is a versatile and commonly used building component. Its uses range from floor systems in office buildings, to speed-ramps in parking structures, to roof systems in stair towers. They are either four-feet or eight-feet wide and can span in length to greater than thirty feet. Photos of the precast planks product are shown in Figure 1.1.

As the name implies, the plank cross-section contains cores or voids normally at four inches on center that run the entire length of the member. These voids are a great weight-saver, but they also make it extremely difficult to cast any inserts into the member. In some building applications, the voids are used for electrical and mechanical runs, or are insulated to reduce sound transmission or heat loss.



Figure 1.1 Yarded Precast Hollow-core Plank

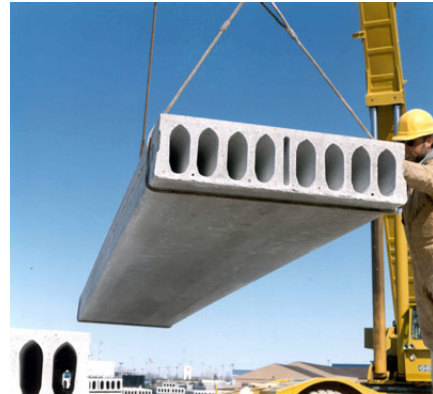


Figure 1.2 Hollow-core Plank Sling-lifted in Yard

Traditionally, the precast planks are reinforced, extruded and left to cure overnight. The next morning, the plank is saw-cut in the form desired, vacuum-lifted

onto a trailer, then sling-lifted into the storage yard. During the erection process, the erector will sling the plank off of the truck, lift it as close as possible to its final position, and remove the slings. The erector must then “muscle” the plank into place using crowbars. The slinging process is shown in Figure 1.2. This process becomes extremely difficult for the last few planks in a floor system and becomes even more time consuming as the plank grows in length and width. The erection of precast hollow core plank in this way can lead to danger on the job site with the resulting increased potential for injury.

There is significant opportunity and need to develop a more efficient and safer method to lift and set hollow-core concrete planks that do not require the use of slings or crowbars to install the precast hollow-core plank members. At present, the most viable option and the focus of this thesis is the use of P-52 “Swift-Lift” Inserts by Dayton Superior installed into the plank using non-shrink grout after casting (i.e. post-installed). “Swift-Lift” inserts are currently an industry-wide method to lift, tilt and erect precast concrete wall panels, spandrels and solid concrete labs. The inserts are small, extremely easy to install, and have excellent tension and shear capacities when installed in solid concrete components. Their use in hollow-core precast planks remains uncertain, relative to their use in solid panels, due to the uncertainty with respect to the capacity of the inserts cast into the top of the cells of the hollow-core plank. Examples of the Dayton Superior product and the lifting mechanism are given in Figures 1.3 through 1.5.

The Dayton Superior inserts have several advantages. All of the inserts use the same universal attachment clasp (Figure 1.5) which allows erectors to use four to eight picking clasps to connect their rigging lines to erect all of the precast panels in a project, making the use of this insert extremely economical. After installation, the insert head can

be easily covered up or hidden if required. Using this insert to lift hollow-core planks would have additional benefits, since the inserts would be installed on the top face of the member and there would be no straps to get in the way. The plank can then be dropped into its final position, released from the rigging and connected to the supporting structure. This reduces the effort and time required to install each plank. Since the inserts are installed on the top face of the plank, the picking head can often be covered up by the topping, flooring or roofing material installed on top of the plank taking minimal effort during construction.



Figure 1.3 Swift-Lift Anchor



Figure 1.4 Picking head of installed Swift-Lift Anchor



Figure 1.5 Insert with engaged picking clasp

1.2 Objectives of Thesis

The first objective of this thesis is to experimentally evaluate the tensile (pull-out) capacity of a 3/4 inch diameter by 5 1/2 inch long “Swift-Lift” headed stud insert, post-installed into precast hollow core planks using non-shrink grout. The second objective is to formulate analytical expressions capable of reliably predicting this tensile (pull-out) capacity of the inserts.

The present research effort includes the design of experimental fixtures which were fabricated and installed in the Marquette University Engineering Materials and Structural Testing Laboratory (EMSTL) along with an MTS actuator mounted to a steel frame to pull the insert out of the plank. The recorded failure load and deflection test data collected is subjected to a statistical evaluation and compared to the predictive equations developed from a review of the existing literature. A recommended capacity will then be derived along with an adequate safety factor for use in the field.

1.3 Outline of Thesis

To achieve the objectives set forth in the previous section, we begin with a literature review and synthesis in Chapter 2. A discussion of the capacities from the handbook and limitations of the Dayton-Superior Product handbook is presented, along with a summary of the design assumptions and procedures present in several versions of the Precast Concrete Institute Design Manual. Finally, the development of predictive equations for pull-out strength is discussed in detail.

Chapter 3 focuses on experimental testing. The insert installation procedure is presented followed by a description of all of the testing equipment and a design check of

all of the testing equipment components. The chapter ends with an explanation of the experimental testing procedure used to perform this research.

Chapter 4 presents the experimental results and a description of the failure mechanisms that were observed during testing. A summary of the measured tensile capacities of all of the inserts tested is provided along with the measured concrete and grout strengths. Finally, a discussion of a statistical analysis performed on the relevant data is presented.

The final chapter presents the findings and conclusions resulting from the research. An outline of the recommendations for any potential future research finishes off the chapter to allow for the potential expansion of the current effort to extend or fine-tune the findings described herein.

Chapter 2

Literature Review and Synthesis

2.0 Introduction

This chapter discusses the research, data and design material that is available to precast concrete manufacturers to size, install and use P-52 inserts in precast members. It also includes a discussion of the assumptions made to analyze the insert and the development of existing equations to predict the tensile capacity of the insert in hollow-core planks.

The literature review will discuss the recommendations presented in the Dayton-Superior Product Handbook and how they apply to the situation currently under consideration. A review of the research efforts used as the basis for PCI design methods will follow along with a discussion of the design procedure presented in several editions of the PCI design manual. A detailed discussion and development of the predictive equation for pull-out strength will follow and conclude the chapter.

2.1 Literature Review

We will begin the literature review by exploring the descriptions and design recommendations presented in the manufacturer's product handbook regarding the design and sizing of inserts cast in concrete. All of the capacities provided in the handbook for these inserts were developed from testing done by an independent company contracted by Dayton-Superior. While no research has been done with inserts post-installed in hollow-core concrete planks, some insight might be obtained from the capacities, illustrations, and data presented in the manual.

Dayton-Superior Product Handbook (Dayton 2011)

Dayton-Superior, along with other insert manufacturers, provide precast suppliers with a handbook describing their available inserts as well as their applications, installation procedure and insert capacities. As mentioned above, the capacities are determined through testing done by an independent testing laboratory and have a safety factor applied to them. The prescribed minimum concrete strength and minimum edge distance used during testing is presented as are any other reduction factors to be applied when sizing the necessary insert.

The P-52 insert is part of the “Swift-Lift” line of lifting inserts offered by Dayton-Superior. The shape of the insert and the fact that there are no coils and no welds necessary to use it, allows industry erectors to attach to and release from any precast piece quickly and efficiently. The attachment hardware can be re-used multiple times and the carbon steel insert complies with all of OSHA’s safety requirements to achieve a safety factor of four.

From the chart presented in the product handbook (see Appendix B), the exact dimensions of the insert are as follows. Figure 2.1 is a schematic of the insert. The overall length of the insert is 5 1/2 inches. Once it is installed, the insert is set down from the top of the plank 1/2 inch, making the overall embedment of the insert approximately six inches. This is achieved by installing the insert with its round plastic recess plug flush with the top of the plank.

Following the recommendations contained in the charts and descriptions presented in the handbook, the expected tensile capacity of the insert is 7,400 lbs, which after removing the 4 to 1 safety factor gives you an ultimate capacity of 29,600 lbs. The

minimum edge distance required to achieve this load is 17 inches. In the case considered in this effort, the maximum edge distance (d_{e1}) is around 8 inches and the minimum (d_{e2}) is $2\frac{7}{8}$ inches. Figure 2.2b is a schematic of the insert with relation to its edge distances.

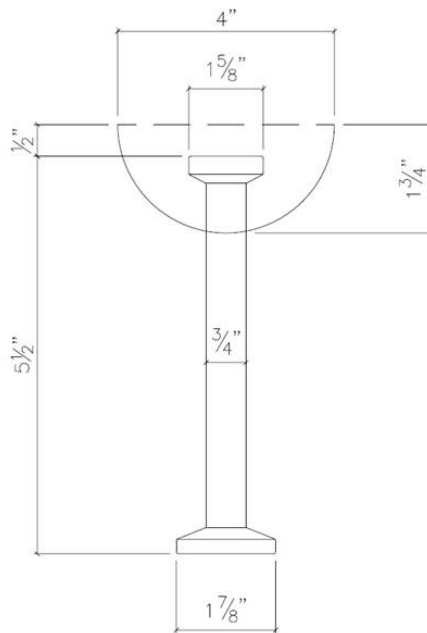


Figure 2.1 P-51 Insert sketch & dimensions

Comparing the edge distances discussed above, it is obvious that the ultimate capacity presented in the handbook likely would not apply. If an insert has a smaller edge distance than what is required, the insert has much less concrete to help resist any load applied to it; therefore the ultimate capacity of the insert is much less. If this insert were a coil insert, Dayton-Superior provides a chart with reduction factors to apply to the base capacity when sizing the insert to account for small edge distances. Unfortunately, no factors are provided for the P-52 inserts considered in the present study. The handbook does provide a chart with the effective tensile capacity of inserts cast at the top

of thin solid concrete walls. This case could be applicable to the insert embedded in hollow-core plank, but again, no data is provided for an insert of similar size. Due to the lack of sizing information in the Handbook (Dayton 2011), additional research and testing is necessary to safely use these inserts in precast hollow-core planks.

All of the schematics and technical information provided in the manual refer to an expected failure in the form of a shear cone normally seen in headed anchor studs cast in solid concrete. Taking into account the shape of the insert, the insert material and the application, a very important assumption is be made in developing design/predictive equations: the inserts act as headed anchor studs (HAS) embedded in concrete; therefore, HAS design equations can be used to model the behavior and estimate the tensile capacity of these inserts. A shear cone is going to be used to analytically estimate the pull-out strength of the insert. Developing a shear-cone analysis procedure and then experimentally evaluating predictive equations for strength based upon these procedures is the goal of the present thesis effort.

2.2.1 PCI Design Handbook

To better understand how to develop an analytical procedure consistent with the common shear-cone model, the Precast/Prestressed Concrete Institute (PCI) Design Handbook was consulted. The handbook is currently in its seventh edition, but focus will be placed on the fourth edition and on the sixth edition for reasons that will be explained in what follows. At the time the fourth edition was published in 1992, very little research had been done in the area of headed anchor stud (HAS) tensile and shear strength. The PCI presented at that time an article with a design procedure for welded-headed studs cast in unconfined concrete (Shaikh and Yi 1985). The authors of the article tested several

headed studs in tension and in shear. Forces directed toward the edge and parallel to the edge of the concrete it was cast in were considered. They also noted the different effects that groups of studs had on both the tensile and shear capacities of the studs. As mentioned before, the design equations presented in the fourth edition were taken exactly from this article without any changes made to them. For purposes of this study, the only equation used is the one pertaining to the tensile capacity of a single headed anchor stud.

Between the fourth and fifth editions, additional research was done and the PCI decided to make some changes to the design equations presented in the fourth edition. While no problems, failures or any other issues had been reported, PCI decided to reduce the shear capacity equations from previous editions, and the equation for the tensile capacity of a group of HAS was reduced by about a third to better represent the findings in the research. Further discussion of these changes can be found in (PCI 1999). The tensile capacity equations for a single headed anchor stud were left unchanged; therefore for the purposes of this effort, the fourth and fifth editions are the same.

By the time of the printing of the sixth edition in 2004, a great deal of research had been done on the subject, and a completely new and much more conservative set of equations were presented. While the PCI emphasizes that there have been no reported incidences of structural failures using any of the previous recommended design equations, they decided to make changes so that their designs would comply with the ACI code requirements (ACI 2005). Therefore, the tensile equations in the sixth edition are based on the equations and recommendations of ACI 318-05 Appendix D. As a result, the calculated design capacity now includes several parameters that were not included in previous design equations. These will be discussed in detail later in the chapter. The

shear capacities for this edition of the PCI manual do not follow the equations of the ACI; instead they are developed using results from testing based on the 5% fractile of the individual anchor strength. Our effort only focuses on the tensile strength, therefore, the shear capacity and the basis of this testing will not be discussed. The headed anchor stud design calculations for both shear and tensile capacity were left unchanged in the 7th edition.

The design equations from the fourth edition and the sixth edition will be discussed and explained in detail in the following sections.

Fourth and Fifth Edition (PCI 1992)

In the fourth and fifth editions of the PCI Design Handbook the design equations are based on the assumption that tensile failure of the headed anchor stud will be based on the shape of a truncated failure cone with a forty-five degree shear plane starting at the outer edge of the foot of the stud. See figure 2.2a for a picture of this failure cone. The design methodology for all PCI equations is to have (whenever possible) a failure mode in which yielding precedes total failure. The reason for this is to have a “warning” of impending failure to minimize any potential loss of life and allowing for the possibility of the removal of any excessive loads to maintain the stability of the structure. In the design of headed anchor studs, the element that should be designed to yield is the steel stud. Unfortunately, due to the limitations of concrete, the limited embedment length, and the ever-increasing need for smaller edge distances, the design of headed anchor studs is more often than not governed by concrete shear failure.

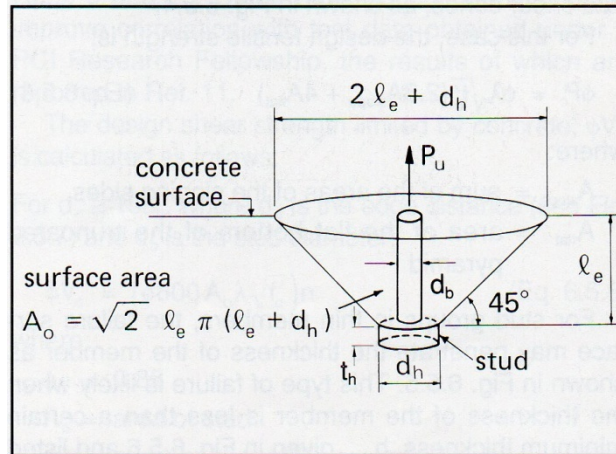


Figure 2.2(a) Concrete surface area of failure cone. (PCI 1992)

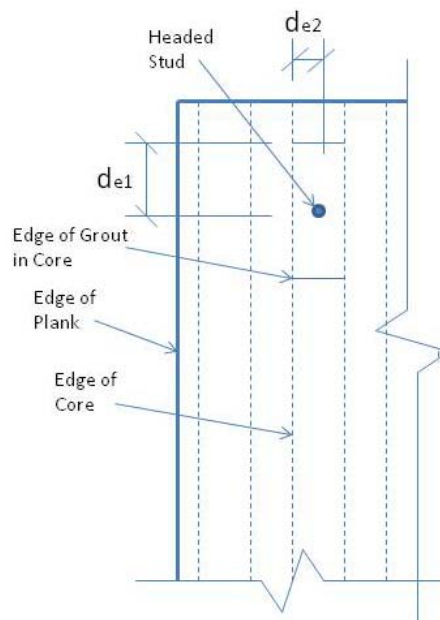


Figure 2.2(b) Plan View of Plank

Using the equations from the fourth edition, the design tensile strength of a headed anchor stud with the same dimensions as the insert we are testing would be determined as follows. First, the surface area of the failure surface needs to be calculated. Using the equation presented in Figure 2.2(a), the surface area of the truncated cone is given by:

$$A_o = (\sqrt{2}) * l_e * \pi * (l_e + d_h) \quad (2.1)$$

where l_e equals the effective embedment length and d_h equals the foot diameter.

The next step is to calculate the edge reduction factors. In our case we will have to calculate two different factors, one for the 8 inch effective edge distance (d_{e1}) and one for an effective edge distance (d_{e2}) equaling 2 7/8 inches. The reduction factor is a ratio of the effective edge distance over the effective embedment length of the insert and cannot be greater than one:

$$C_{e1} = \frac{d_{e1}}{l_e} \leq 1 \quad (2.2)$$

$$C_{e2} = \frac{d_{e2}}{l_e} \leq 1 \quad (2.2a)$$

Finally, the third step is to calculate the tensile capacity.

$$P_c = C_{e1} * C_{e2} * A_o * (2.8) * \lambda * \sqrt{f'_c} \quad (2.3)$$

where λ is a light weight concrete factor, and f'_c is the concrete unconfined compression strength in pounds per square inch (psi).

Filling in all of the equations for the insert considered results in the following:

$$A_o = (\sqrt{2}) * 6" * \pi * (6" + 1.875") = 209.93 \text{ in}^2$$

$$C_{e1} = 8"/6" = 1.3333 > 1 \therefore C_{e1} = 1$$

$$C_{e2} = 2.875"/6" = 0.48$$

$$P_c = 1 * 0.48 * 209.93 \text{ in}^2 * 2.8 * 1 * \sqrt{3000} = 15,454 \text{ lbs}$$

It is important to note that in normal designs, the tensile capacity is multiplied by an additional factor ($\phi = 0.85$) to give the design capacity. The failure load (strength limit state) is being computed, so the phi factor does not need to be applied.

Sixth Edition (PCI 2004)

The goal of the design methodology in the sixth and seventh edition is the same as the fourth edition, but the assumptions and equations used to achieve this are now completely different. In this edition, the design of the tensile strength of headed anchor studs is divided into three failure modes; breakout [ϕN_{cb}], pullout [ϕN_{pn}] and side-face blowout [ϕN_{sb}]. The smallest of these three modes will control the capacity of the anchor. Additional discussion of the failure modes, beyond of what is discussed below, is available in (PCI 2004) and the resources therein.

The concrete breakout strength [N_{cb}] is usually the most critical and is very similar to the failure mode that is discussed in the fourth edition. One critical difference though, is the fact that the assumed failure angle is 35 degrees from the horizontal. The equation for the concrete breakout strength is as follows:

$$N_{cb} = C_{bs} * A_n * C_{crb} * \Psi_{ed,N} \quad (2.4)$$

Where the breakout strength coefficient is equal to:

$$C_{bs} = 3.33 * \lambda * \sqrt{\frac{f'_c}{h_{ef}}} \quad (2.5)$$

λ is the light weight concrete factor, f'_c is the concrete strength and h_{ef} is the effective embedment depth of the stud. If the maximum edge distance of the anchor is less than h_{ef} divided by 1.5, then the effective embedment depth will be limited to h_{ef} divided by 1.5. A_n is the projected surface area for the stud. C_{crb} is the concrete cracking factor, usually 1.0 and $\Psi_{ed,N}$ is the edge distance factor. The equation for $\Psi_{ed,N}$ is;

$$\Psi_{ed,N} = 0.7 + 0.3 \left(\frac{d_{e,min}}{1.5 h_{ef}} \right) \leq 1.0 \quad (2.6)$$

The concrete pullout strength $[N_{pn}]$ is a measure of the behavior of the bearing of the stud head against the concrete. The equation used to predict this strength is,

$$N_{pn} = 11.2 * A_{brg} * f'_c * C_{crp} \quad (2.7)$$

A_{brg} is the bearing area of the stud head that is in contact with the concrete while tension is applied, and C_{crp} is the concrete cracking factor, usually 1.0.

There are two considerations for the side-face blowout strength $[N_{sb}]$. If the smallest edge distance is less than forty-percent of the effective embedment depth ($d_{e1} < 0.4h_{ef}$), then

$$N_{sb} = 160 * d_{e1} * \sqrt{A_{brg}} * \sqrt{f'_c} \quad (2.8)$$

If the stud is located at a perpendicular distance (d_{e2}) that is less than three times the smallest edge distance (d_{e1}), then the above equation is multiplied by: $(1 + \frac{d_{e2}}{d_{e1}})/4$, where the ratio of d_{e2} to d_{e1} is between 1 and 3.

Evaluating the three limit states for the inserts and configuration considered in this research effort results in the following:

-Concrete Breakout Strength:

$$h_{ef} = 6" > \frac{8"}{1.5} = 5.33" \therefore h_{ef} = 5.33"$$

$$C_{bs} = 3.33 * 1.0 * \sqrt{\frac{3,000psi}{5.33"}} = 79.0$$

$$A_n = (2.875" + 2.875") * (8" + 8") = 92 \text{ in}^2$$

$$\Psi_{ed,N} = 0.7 + 0.3 \left(\frac{2.875"}{1.5 * 5.33"} \right) = 0.808$$

$$N_{cb} = 79.0 * 92 * 1 * 0.808 = 5,873 \text{ lbs}$$

-Concrete Pullout Strength:

$$N_{pn} = 11.2 * (\pi * (1.875" - 0.75")) * 3,000psi * 1.0 = 118,752 \text{ lbs}$$

-Side-Face Blowout Strength:

In the case we are studying, d_{e1} equals 2.875" and d_{e2} equals 8".

$$N_{sb} = 160 * 2.875 * \sqrt{(\pi * (1.875" - 0.75")) * 3000} * \frac{1 + \left(\frac{8}{2.875}\right)}{4} = 44,765 \text{ lb}$$

As previously discussed, the controlling tensile capacity of the headed anchor stud is the minimum value of the three calculated failure modes that are discussed in the sixth and seventh edition of the PCI manual. The minimum of these gives us a tensile capacity of the stud of 5.9 kips governed by the breakout strength of the stud. As in the 4th edition of the PCI, this value would be multiplied by a phi factor, in this case equaling 0.75, but since we require the failure capacity of the HAS, the safety factor will be omitted.

2.2 Predictive Equation for Pull-Out Strength

Comparing the results from the fourth edition (PCI 1992) and sixth edition (PCI 2004), several observations can be made. First and more importantly, there is a 260% difference in the capacities obtained from these two design methodologies. The 5,900 lb capacity obtained from the sixth edition seems very low compared to the 15,000 lb capacity from the fourth edition. Comparing these two numbers to the unreduced capacity of over 29,000 lbs obtained from the Dayton Superior manual, it will be assumed that the results obtained following the design methodology of the 4th edition are more accurate than the 6th edition for obtaining the true capacity of the inserts.

One can compare results to some values provided by the Dayton Superior manual. Figure 2.4 (Dayton 2011) illustrates the capacity of a 4-ton by 9 1/2" long insert cast into

the top edge of thin precast walls at various distances from the corner. The actual minimum edge distance of the insert tested in this study is 2 7/8". For the purposes of this discussion, we will use d_e equal to 3". Using the smallest corner distance of 10", a concrete strength of 4500 psi and a 6" effective wall thickness, the safe tensile capacity equals 4,000 pounds. Taking away the four-to-one safety factor and ignoring the difference in concrete strengths, the insert capacity equals:

$$4,000 * 4 = 16,000 \text{ lbs}$$

Repeating the same procedure for the 15" corner distance, we get a capacity of nineteen thousand pounds [$4 * 4,800 \text{ lbs} = 19,200 \text{ lbs}$]. Comparing these capacities to the capacity calculated using the fourth edition (Eq. 2.3), it can be seen that the previous assumptions of treating the insert as a headed anchor stud are correct. The insert in the plank, is cast into a 16" long section of grout, 16" away from the edge of the plank; therefore, the actual corner edge distance could be argued to be between 8" and 16".

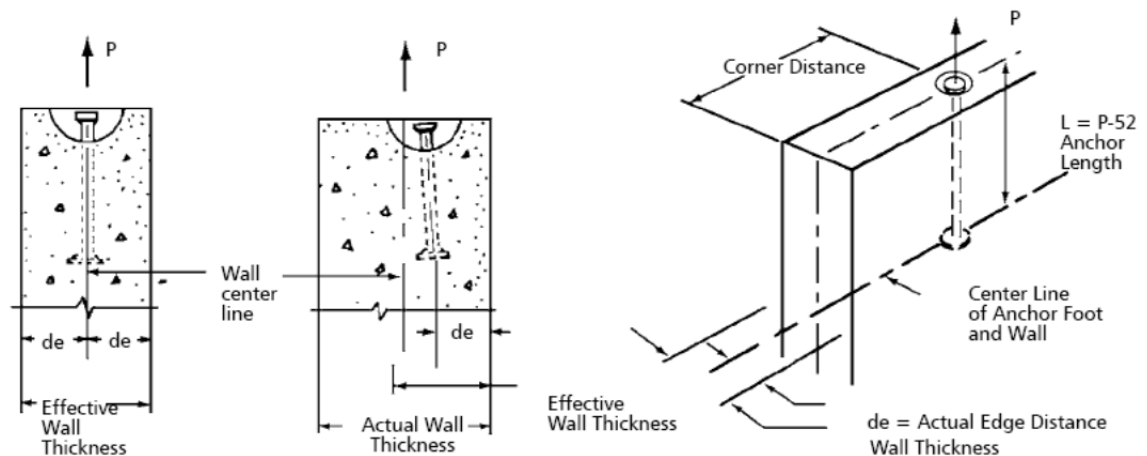


Figure 2.3 Illustration, P-52 Insert Cast into top of thin walls. [Dayton 2011, p.31]

| Swift Lift Anchor Tons x Length | Effective Wall Thickness 2 de | Actual Edge Distance de | Tensile Safe Working Load Per Anchor | | | | |
|--|--|----------------------------------|--------------------------------------|------------|------------|------------|------------|
| | | | Actual Corner Distance | | | | |
| | | | 10" | 15" | 20" | 24" | 30" |
| 4 Tons x 9-1/2" Long | 3-3/4" | 1-7/8" | 2,500 lbs. | 3,000 lbs. | 3,300 lbs. | 3,400 lbs. | 3,500 lbs. |
| | 4" | 2" | 2,600 lbs. | 3,200 lbs. | 3,500 lbs. | 3,700 lbs. | 3,800 lbs. |
| | 5" | 2-1/2" | 3,300 lbs. | 4,000 lbs. | 4,400 lbs. | 4,600 lbs. | 4,700 lbs. |
| | 6" | 3" | 4,000 lbs. | 4,800 lbs. | 5,300 lbs. | 5,500 lbs. | 5,700 lbs. |
| | 7" | 3-1/2" | 4,700 lbs. | 5,600 lbs. | 6,200 lbs. | 6,500 lbs. | 6,600 lbs. |
| | 8" | 4" | 5,300 lbs. | 6,400 lbs. | 7,000 lbs. | 7,400 lbs. | 7,600 lbs. |

Figure 2.4 Tensile Safe Working Load for Anchors Cast in Thin Walls ($f'_c = 4.5$ ksi) [Dayton 2011, p.32]

To create a predictive equation, the equations from the fourth edition of the PCI HAS design (PCI 1992) will be adopted. The same design methodology is being used here with an exception. Instead of using 45 degrees as the assumed angle of the pullout cone, we will run the calculations using 30, 35, 40, 45, 50, 55 and 60 degrees. The fourth edition uses a ratio of the edge distance to the effective length (Eq. 2-2) to reduce the area of the assumed failure surface in each edge direction. Three-dimensional modeling software (in our case Google Sketchup) is used to model the area of the failure surface at each of the above mentioned angles. The area consists of three different sections. The first section is full height section of the cone between the cores. The second section is the smaller section of cone cut by the cores on either side of the insert. The third section is the area between the top of the core and the top of the plank. Figure 2.5a and Figure 2.5b show two section views of the plank and insert to better visualize the three areas described above.

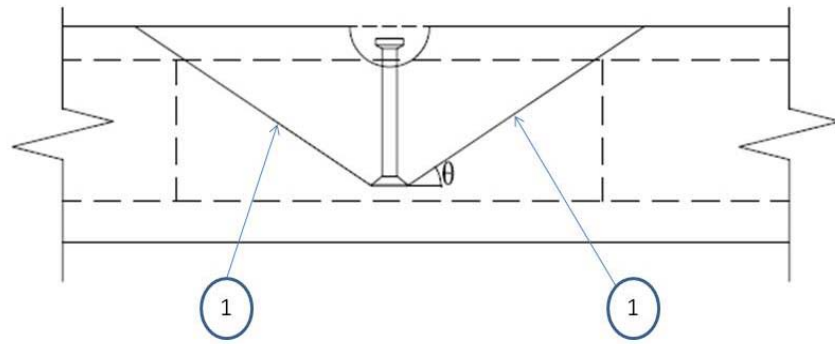


Figure 2.5a Failure cone area section 1

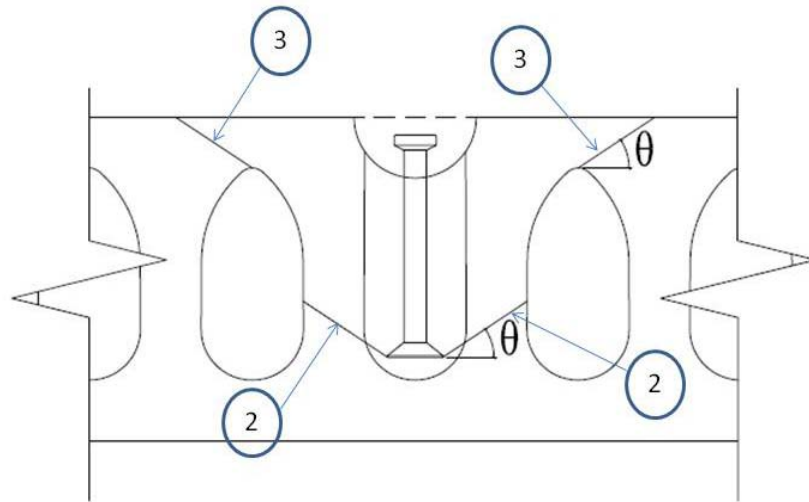


Figure 2.5b Failure cone area sections 2 & 3

Once these areas are calculated, they will then be plugged into Eq. 2.3, and $Ce1$ and $Ce2$ are set equal to 1. The concrete strength will be taken as 3,000 psi and adjusted if necessary to account for the concrete and grout strengths determined during testing. Summarizing these calculations:

Table 2.1 Predictive equation calculation summary.

| Angle (θ) (Deg.) | Ao [in ²] | Pc 1 (PCI 1992) [lb.] |
|------------------------------|--------------------------|--------------------------|
| 30 | 80.09 | 12,283 |
| 35 | 80.43 | 12,334 |
| 40 | 73.95 | 11,341 |
| 45 | 69.30 | 10,628 |
| 50 | 66.89 | 10,258 |
| 55 | 68.45 | 10,498 |
| 60 | 72.046 | 11,049 |

Chapter 3

Experimental Testing

3.0 Introduction

Sixteen P-52 “Swift-Lift” Inserts by Dayton-Superior installed in four precast hollow-core concrete planks were tested to failure in this research. Four inserts were installed in each eleven foot long plank, and a total of four planks were used to conduct and complete this research. This chapter discusses in detail the procedure and materials that were used to create all four specimens, along with the experimental testing method used throughout this research.

3.1 Precast Hollow-Core Plank and Insert Installation

This section describes the production procedure of the Hollow-Core Plank performed at the Spancrete Inc. precast plant in Valders Wisconsin, and the method used to cast the inserts into the precast hollow-core plank.

The precast planks used in this research effort used twenty-four (24) 7/16” dia. 270 ksi low-relaxation prestressing strands stressed at 75% of the f_{pu} , and placed 0.75” from the bottom of the plank. They were fabricated using concrete with a target 28-day unconfined compression strength of 6,000 psi and an unconfined compression strength at release targeted to be 3,500 psi.

During the production process, the strands are first laid out across the casting bed and stressed. The extruding machine then runs along the casting bed and places the concrete. As part of the placing process, the dry-pack concrete is automatically compacted and formed in the shape of the plank with hollow voids. As soon as the extruding machine goes past a location where an insert was to be installed, the extruder

operator cuts out a 4" by 16" opening centered over a core as shown in Figure 3.1. Since the concrete is still "wet", this process takes minimal effort and the tool required to do the job is analogous to a large putty knife. This is one of the main reasons this is done as soon as the extruder goes by. If this process is delayed, cutting the opening could not only cause extensive damage to the plank, but would require concrete sawing equipment. Another good reason to cut and install the insert while the concrete is still "wet" is to avoid forming a cold joint between the concrete and the grout around the insert. This allows for better adhesion between the two materials and potentially a higher insert capacity. An appreciation of scale can be seen in Figures 3.1 and 3.2 where the headed insert is shown adjacent to the slot made in the plank.



Figure 3.1 Opening in Precast Hollow-Core Plank



Figure 3.2 Opening & Insert prior to Installation

Non-shrink grout with 28-day target unconfined compression strength of 3,000 psi is then poured in the opening and leveled off at the top of the plank with the insert. The process is schematically shown in Figures 3.3 and 3.4. The insert and its plastic spherical cap are then pushed into the center of the opening. This process is then repeated until all inserts were installed. It is important to note that once the plastic cap is removed, the five and a half inch long insert ends up set down one half inch ($1/2''$) from

the top of the plank and gives the insert a total embedment of six inches, thus placing the bottom of the insert directly at the bottom of the core in the plank.



Figure 3.3 Grout Installation



Figure 3.4 Insert Installation

The next morning, the planks are cut with a concrete saw to the correct length. The planks were then placed on a trailer using a vacuum picker and taken to the yard for storage. No more than 5 days later the planks were shipped to Marquette University for testing.

3.2 Experimental Fixturing and Testing Protocol

This section describes the experimental fixturing (including design of the testing fixtures) and testing protocols used for this research.

Experimental Fixture

The testing fixture used at Marquette University in the Engineering Materials and Structural Testing Laboratory (EMSTL) consists of an eleven and a half foot long W12x72 beam supported by two ten foot long W12x72 columns. The configuration of this structural steel fixture is shown in Figure 3.5. The ends of the beam are welded to a half inch thick end plate using quarter inch weld. The end plates are bolted to the flange of the W12x72 column, using six (6) five-eighths inch diameter bolts. The base of the

column is also welded to a half inch thick base plate using quarter inch weld, which is then attached to the concrete strong-floor using one inch diameter threaded rods (through the strong-floor). An MTS single ended hydraulic actuator with a tensile capacity of thirty-six kips is bolted to the beam along with the angles and swift-lift attachment that were used to pull on the insert during testing. The actuator is connected to a computer which controls the actuator & records the tensile force and deflection of the insert at failure using software written in MTS Testworks Software.

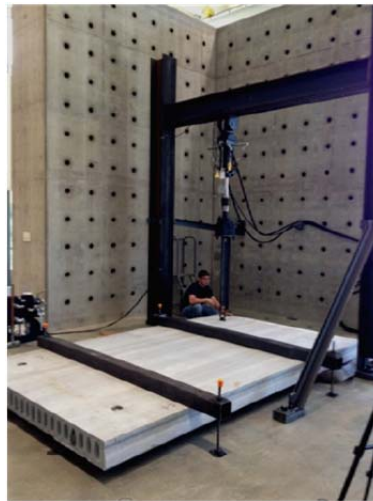


Figure 3.5 Plank and Testing Equipment



Figure 3.6 Plank and Testing Equipment



Figure 3.7 Plank and Testing Equipment (Side view)

The precast plank specimens were stored in the Marquette University EMSTL until testing and are moved using slings attached to the laboratory's overhead crane. During testing, the plank is placed on two pairs of four foot long two-by-fours and is centered within the testing frame with the P-52 insert directly underneath the actuator. Shims are located at fifty-two inches from the testing end and thirteen-foot three inches from the testing end in order to minimize the upward force on the tie-down beam closest to the testing end. Two "hold-down" beams are placed on the plank. One is placed three feet away from the insert and is the only beam that will hold down the plank during testing. The second tie-down beam is not needed for testing, but was added to keep the plank from shifting or sliding during testing. The "hold-down" beams consisted of a ten-foot long HSS 5x5x1/2. The beams are held down by a single one inch diameter threaded rod at each end, thru-bolted to the floor.

Testing Protocol

The testing procedure for this effort was very straight forward, but in an effort to limit having to move the actuator only once, the inserts were not tested in order. Two inserts in each plank were tested, at opposite corners, then the actuator was moved. After the move, the other half of the inserts were tested.

As mentioned above, each plank was moved into place using two slings and the over-head crane. In an effort to reduce any eccentric or angled load on the insert, a plumb-bob was used to place the plank so that the insert was directly below the actuator. Once the plank was in place, the "hold-down" beams were installed and attached to the strong floor. The lifting clasp was engaged on the insert and attached to the actuator. The actuator is then engaged and the insert was then loaded to four-hundred pounds to take

the “slack” out of the system. A new data file in the actuator program was created and labeled to match the insert being tested.

Several important parameters were set for each trial; the rate of loading application; how to apply and record the load on the system, the data sampling rate and the test termination criterion. The load was applied to the insert by enforcing a set displacement for the actuator head and recording the load measured in the actuator to achieve the displacement. The rate used to run the first half of the tests was 0.05 inches per minute. This means that the actuator head moved vertically 0.05 inches every minute, and the load was recorded five times every second. After half the inserts were tested, the rate was tripled to 0.15” in order to shorten the testing time, but the load was still recorded five times every second. The loading rate was still very slow, and none of the results seemed to be affected by the rate change. In order to avoid a catastrophic or very destructive failure in the lab, the test was set to stop once the recorded load dropped below ninety percent of the maximum recorded load. Since the plank was over-designed to resist any flexural loads and the steel tensile capacity of the insert is much higher than the expected insert capacity, the system failure was expected to be brittle. Therefore a ten percent drop in recorded load would be enough of a buffer to record the maximum load, the small decrease in load that normally happens just prior to failure and the sudden drop in load at failure.

Once the parameters were set, the actuator was activated and the tensile force was slowly increased on the system until the insert or the plank failed. After failure, the failure mode seen in the specimen was determined and recorded along with the ultimate

deflection and maximum experienced tensile force. The equipment was then un-hooked and the plank was removed. This procedure was repeated until all inserts were tested.

The test results were then summarized and analyzed in Excel. Following a statistical analysis, the results were then compared to the predictive equations derived in Chapter two and a recommended insert capacity was determined. A detailed discussion of the analysis of the test results and recommendations can be found in Chapters Four and Five respectively.

3.2 Experimental Fixture Design

This section outlines the procedure that was used to verify the adequacy of the testing equipment and the design of the precast plank specimen that was used during the experimental testing. The insert capacity stated in the Dayton Superior Product Handbook (Dayton 2011) is 7,400 pounds (Appendix C). After removing the safety factor of four, the capacity is 30 kips. As it was previously stated in chapter two, the edge distances around the insert are smaller than the edge distances presented in the handbook; therefore this number does not apply directly. Knowing that the load will not reach its maximum load, we can conservatively take the handbook capacity as the ultimate load and not apply any amplification factor (load factor) to this load giving,

$$T = 30 \text{ Kips}$$

This will be the maximum applied load [T] used for all of the following calculations. It should be noted the experimental fixtures were previously sized to be used at the testing laboratory in several different applications beyond the requirements of this particular effort. The calculations done in this chapter are done to verify the adequacy of such equipment for use in this testing program.

Concrete Precast Hollow-Core Plank Design

The present section will outline the design of the precast plank test specimen to be used as the basis for the present research effort.

Using Figure 3.8, one can analyze the loads on the plank and find the maximum moment as:

$$M_u = 30 \text{ Kips} * 3.0' = 90 \text{ Kip} - ft$$

Spancrete Inc. has plank design charts (see Appendix A) to aid engineers in designing planks with simple loadings. All of their plank charts are for four-foot wide planks, but when an eight foot wide plank is required the strand pattern is doubled in the design. Plank design 0.75F-8712 has a moment capacity of 42.64 Kip-ft per foot. The maximum moment occurs at the tie-down spot (four foot-four inches from the end). Since the strand requires about seven feet to fully develop, the moment capacity can be reduced by the ratio of the distance to the spot of maximum load to the distance the strand requires to develop. Assuming half the plank width (four feet of plank) takes the load and reducing the moment capacity by the above mentioned ratio, the capacity of the plank is:

$$\phi M_n = 42.64 \frac{\text{Kip-ft}}{\text{ft}} * 4' - 0" = 170.6 \text{ Kip} - ft * (4.5'/7') = 109.6 \text{ Kip} - ft \text{ [OK]}$$

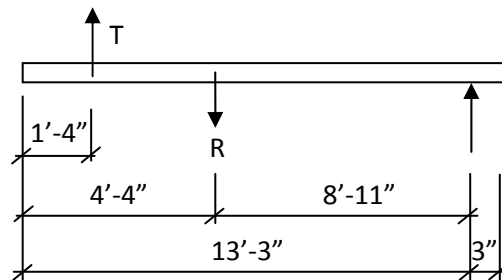


Figure 3.8 Plank Layout Sketch

To summarize, the selected plank is an eight-foot wide [H series], eight inch thick plank with twenty-four, seven-sixteenth inch diameter, two-hundred seventy kip-per-square inch Low-Lax (relaxation) steel strands with three quarters of inch concrete cover. [0.75H-8724]. It is expected that the insert will pull out prior to flexural failure of the plank.

Tie-Down Beam and Anchor Design

The maximum hold-down force [R] as a result of the insert loading can be computed using the free body diagram in Figure 3.8. Summing moments gives the hold down force:

$$R = \frac{30 \text{ Kips} * (8.917' + 3.0')}{8.917'} = 40.1 \text{ Kips}$$

The free body diagram shown in Figure 3.9 can be used to determine the necessary dimensions and size for the fixture tie-down beam. In order to model the fact that the insert is located closer to the side of the plank and as such, when the tensile force is applied, the load on the tie-down beam will not be symmetrical; it was assumed that 2/3 of the tensile force was applied to one side of the plank, and 1/3 was applied to the other side.

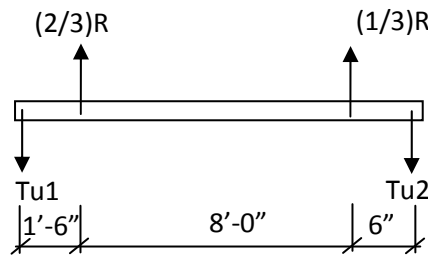


Figure 3.9 Tie-Down Beam Layout

The maximum uplift force [T_{u1}] and the maximum moment on the beam [M_u] can be determined with reference to Figure 3.9 as follows:

$$T_{u1} = \frac{\left(\frac{2}{3}\right) * 40.1 \text{ Kips} * (8.5') + \left(\frac{1}{3}\right) * 40.1 \text{ Kips} * 0.5'}{10'} = 23.4 \text{ Kips}$$

$$M_u = 23.4 \text{ Kips} * 1.5' = 35.1 \text{ Kip} - ft = 421.1 \text{ Kip} - in$$

The tie-down beam can be selected using the target bending moment and it was determined that a steel HSS 5x5x1/2 and 10-ft long with an expected yield strength of 46 ksi would likely be adequate. The preliminary member can now be checked to evaluate its adequacy in shear and bending moment.

Moment Check:

$$Z_{req} = \frac{421.1 \text{ Kip} - in}{0.9 * 46 \text{ Ksi}} = 10.2 \text{ in}^3 < Z_{prov} = 13.1 \text{ in}^3 \text{ [OK]}$$

Shear Check: [$k_v = 5$]

$$1.1 * \sqrt{\frac{5 * 29000 \text{ Ksi}}{46 \text{ Ksi}}} = 61.76 > \frac{h}{t_w} = 7.75 \text{ Therefore } C_v = 1$$

$$\phi V_n = 0.9 * 0.6 * 46 \text{ Ksi} * 2.75" * 2 * 0.465" = 63.53 \text{ Kips} > T_u = 23.4 \text{ Kips [OK]}$$

Finally, we can check the anchor rods attaching the tie-down beam to the floor. Using the AISC Steel Construction manual (AISC 2010), the tensile capacity of a one inch diameter rod made out of an assumed grade of A325 steel is 53 kips which is also greater than the 23 kips calculated above.

Actuator Anchorage Design

The steel frame used to support the actuator consisted of two columns and one beam, all made up of W12x72 steel shapes. Using Figure 3.10 we can compute the maximum moment, expected deflection and shear on the W12x72 shape found in the experimental fixture. The worst case scenario for deflection is considered by placing the load at

midspan. However, the fixture was checked with the actuator positioned 4'-0" from the column centerline.

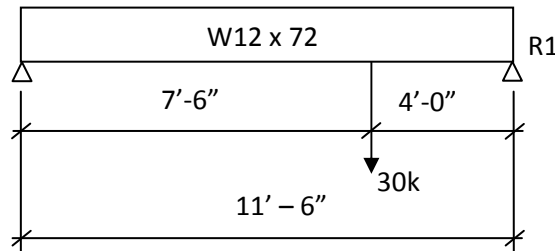


Figure 3.10 Steel Frame, Beam Layout

$$M_u = (30 \text{ Kips}) * \frac{(7.5 \text{ ft} * 4 \text{ ft})}{11.5 \text{ ft}} = 78.3 \text{ K} - \text{ft}$$

$$Z_{req} = \frac{\left[(78.3 \text{ K} - \text{ft}) * \left(12 \frac{\text{in}}{\text{ft}} \right) \right]}{(0.9) * (50 \text{ Ksi})} = 20.9 \text{ in}^3 < Z_{prov} = 108 \text{ in}^3 \text{ [OK]}$$

$$\Delta = \frac{[(30 \text{ Kips}) * (11.5 \text{ ft} * 12)^3]}{[(48) * (29000 \text{ Ksi}) * (597 \text{ in}^4)]} = 0.095 \text{ in}$$

$$\begin{aligned} V_u &= 30 \text{ Kips} < \phi V_n = (0.75) * (0.6) * (50 \text{ Ksi}) * (0.43 \text{ in}) * (9.125 \text{ in}) \\ &= 88.3 \text{ Kips [OK]} \end{aligned}$$

$$R1 = (30 \text{ Kips}) * \frac{(7.5 \text{ ft})}{11.5 \text{ ft}} = 19.57 \text{ Kips}$$

The maximum reaction at the end of the beam (R1) can now be used to check the beam to column connection and the column itself.

Beam to Column Connection

The W12x72 steel beams are attached to the columns using welds from the beam to the end plate and bolts from the end plate to the column. The shear check for the two connection components are as follows:

-Weld from beam to end-plate: [1/4" weld @ beam]

$$\begin{aligned}\phi R_n &= (9.125 \text{ in}) * (2 \text{ welds}) * \left(5.54 \frac{\text{Kips}}{\text{in}}\right) = 101 \text{ Kips} > V_u \\ &= 19.57 \text{ Kips [OK]}\end{aligned}$$

-Bolts from end-plate to column:

$$\begin{aligned}V \text{ per bolt} &= \frac{19.57 \text{ Kips}}{6 \text{ bolts}} = 3.3 \text{ Kips} \\ \phi V_n \text{ bolt} &= 11.0 \text{ Kips} - [\text{Using (6) A325 } 5/8" \text{ Dia. bolts}] > V_u \\ &= 3.3 \text{ Kips [OK]}\end{aligned}$$

Column Check

The last major component to check is the column. The base of the column is welded to the end bearing plate and bolted to the floor.

-Axial Compressive Strength: [W12x72]

$$KL = 12 \text{ ft}$$

$$\phi P_n = 807 \text{ Kips} > P_u = 19.57 \text{ Kips [OK]}$$

K = 1.0 was used and is conservative due to mid-height bracing on vertical columns.

-Axial Tensile Capacity:

$$\phi T_n = 949 \text{ Kips} > T_u = 19.57 \text{ Kips [OK]}$$

-End-Plate Check:

-Column to End-Plate: Weld Capacity [1/4" weld]

$$\begin{aligned}\phi R_n &= (9.125" * 2 \text{ sides}) * (5.54 \text{ Kips/in.}) = 101.1 \text{ Kips} > T_u \\ &= 19.57 \text{ Kips [OK]}\end{aligned}$$

-Bolt check: [(4) 5/8" Dia. Bolts]

$$T_u \text{ per bolt} = \frac{19.57 \text{ Kips}}{4 \text{ bolts}} = 3.3 \text{ Kips} < \phi T_n \text{ bolt} = 20.7 \text{ Kips [OK]}$$

-End-Plate Bending: [PL. $\frac{3}{4}$ " x 15" x 15"]

$$Z_{prov} = \frac{(15"/2) * (\sqrt{2}) * (0.75)^2}{4} = 1.49 \text{ in}^3$$

$$\begin{aligned} \phi P_n &= \frac{(0.9) * (36 \text{ Ksi}) * (1.49 \text{ in}^3)}{3.25 \text{ in.}} = 14.85 \text{ Kips} * (4 \text{ bolts}) = 59.42 \text{ Kips} > P_u \\ &= 19.57 \text{ Kips [OK]} \end{aligned}$$

Finally, the connection to the actuator is checked,

- Bolt Check: [(4)1" Dia. Bolts]

$$T_u \text{ per bolt} = \frac{30 \text{ Kips}}{4} = 7.5 \text{ Kips} < \phi T_n \text{ bolt} = 53 \text{ Kips [OK]}$$

-Weld from PL. $\frac{3}{4}$ "x10 $\frac{1}{4}$ "x10 $\frac{1}{4}$ " to PL. $\frac{3}{4}$ "x3 $\frac{1}{2}$ "x4" w/ hole:

$$\phi R_n = 8" * 5.54 \text{ Kip/in} = 44.32 \text{ Kips} > T_u = 30 \text{ Kips [OK]}$$

-Bearing on $\frac{3}{4}$ " Dia. Hole on PL. $\frac{3}{4}$ "x3 $\frac{1}{2}$ "x4": [Tbl. 7-6]

$$\phi V_n \text{ of } 3/4" \phi \text{ hole} = 44 \text{ Kips}$$

$$[l_e \text{ (actual)} = 1 \frac{1}{2}" ; l_e \text{ (design)} = 1 \frac{1}{4}"] \text{ [OK]}$$

-Shear capacity of $\frac{3}{4}$ " Dia. Bolt: [Tbl. 7-1]

$$\phi V_n \text{ of } 3/4" \phi \text{ bolt} = 24.5 \text{ Kips}$$

The capacity of the bolt is not larger than the factored maximum load [$T_u = 30$ Kips], but if you remove the twenty-five percent reduction, the shear capacity of the bolt is 32.7 Kips. Knowing that the tensile capacity of the insert is well below the thirty kips used in the calculations, the minimal numerical safety factor for this element of the system should suffice for the purposes of this effort.

Chapter 4

Experimental Results and Discussion

4.0 Introduction

This chapter presents the results and failure descriptions of each insert tested. A summary of all of the measured capacities along with a mean is presented at the end of the chapter. Each insert that was tested was labeled with two numbers. The first number represents one of the four planks we tested which were numbered one through four. The second number represents each insert within each of those planks which was also numbered one through four. [e.g. Insert 2 in plank 1 is Insert 1-2.]

It should be noted that to prevent a complete insert pullout, the tensile test was set to stop once the load reached a ten percent reduction of the maximum recorded load. This parameter was set to prevent damage to the system if load was continued to be applied once the initial failure occurred. Once the maximum load was reached, the load in the system would never be higher than the peak load already recorded.

It should also be noted, in setting up planks one and two, a longitudinal crack running the length of the plank along the top developed once the two hold-down beams were placed and tightened. The crack occurred one core over from the center core and ran vertically from the top of the plank to a spot near the top of the core. See Figure 4.1 for a picture of this crack. To avoid this from reoccurring, two-by-fours were placed between the hold-down beam and the top of the plank to distribute the tie-down force more evenly across the width of the plank instead of near the edge. See Figures 4.2 and 4.3 for the two setups used for testing.

4.1 Experimental Failure Modes

As expected from all of the predictive equations, none of the tested inserts failed due to steel yielding or fracturing. All of the failures were concrete failures. Three main types of concrete failures were observed and are labeled as Type A, Type B & Type C. Each of these are discussed below.



Figure 4.1 Longitudinal crack in Hollow-Core Plank **Figure 4.2** Initial setup: Hold-down beam on plank



Figure 4.3 Adjusted setup: Hold-down beam on two by four

Type A- Pullout Cone Extending to Plank End

The four tests observed with Type A failure showed a pullout cone typically crossing at least two cores, one on either side of the core where the insert was cast. The bottom of the cone started at the bottom of the core with the insert. It crossed the web on each side of the core and crossed one more pair of webs also at about the same angle. Beyond that

web, the cone usually came out near the top of the core. See Figures 4.4 to 4.6 for pictures of this cone [Note: the arrow depicts the edge of the failure cone]. Along the length, the pullout cone was approximately 3'-0" to 3'-6" long centered on the insert. Failure Type A appears to deviate from the shear cone assumed in the derivation of the predictive equations in the fact that it is an elongated enough to extend to the plank end.



Figure 4.4 Insert S3-3, Plan View [Failure Mode A] **Figure 4.5** Insert S3-3, Side View [Failure Mode A]



Figure 4.6 Insert S2-2, Plan View [Failure Mode A] **Figure 4.7** Insert S2-2, Side View [Failure Mode A]

Type C- Pull-out Cone

Type C failure was observed in six tests, and the failure began at the insert location. For this failure, a pullout cone was observed, and soon after the plank seems to have split or

separated right at the insert location. In most cases, the crack that was formed ran along the length of the plank, typically splitting around the top of the core where the insert was cast. In a few instances, transverse crack also formed starting at the insert location. See Figures 4.8 and 4.9 for pictures of this failure. Failure mode C appeared to have the closest resemblance to a shear cone failure in the immediate vicinity of the insert assumed in the derivation of the predictive equation for pull-out capacity.



Figure 4.8 Insert S1-3 [Failure Mode C]

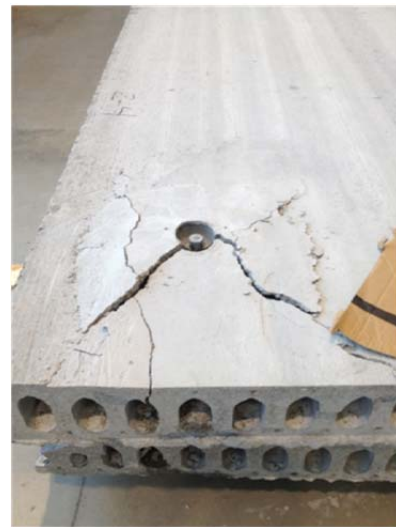


Figure 4.9 Insert S2-4 [Failure Mode C]

Type B- Flat Pullout Cone Splitting at Insert

Type B failure is a combination of Types A and C and is shown in Figures 4.10 and 4.11. Failure Type B is close to Type C with regard to shear cone formation, but in these three observed cases, a very flat pullout cone developed at the bottom of the core where the insert was cast, and it extended across three webs. As the cone was failing, it then seems to have split near the insert causing more damage than in the other two failure types.

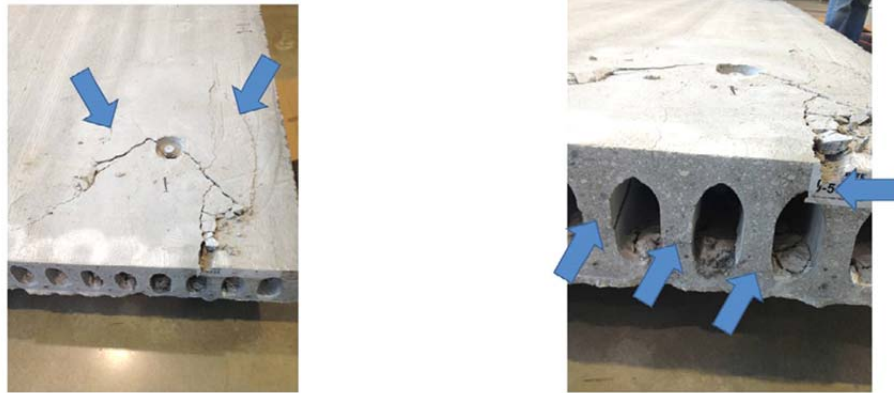


Figure 4.10 Insert S1-1, Plan View [Failure Mode B] **Figure 4.11** Insert S1-1, Side View [Failure Mode B]

Other Failures

Types A, B and C encompass thirteen of the sixteen tests completed. The remaining three tests have additional circumstances which require explanation. Failure Types D and E apply to inserts S3-4 and S4-4, respectively. The concrete around both of these inserts had been damaged by a continuous longitudinal crack that had developed when testing the insert at the opposite end of the plank (S3-1 and S4-1). Insert S3-4 was tested to failure despite the damage and the failure seen is shown in Figures 4.12 and 4.13. The capacity for these was much lower than all of the other inserts, and the damage to the plank was very severe. The test culminated with a section of the plank breaking in half. To avoid another severely damaged plank and knowing that the insert was already compromised, insert S4-4 was not tested.

The final insert failure to be discussed is failure Type F, applying to insert S4-2. Failure for this insert began as a shear failure of the plank one core over from the insert. A vertical crack developed above and below the center of the core and spread along the length of the plank to the hold-down beam. At that point the plank then began to bend failed in flexure at the beam, which triggered the end of the test. No other damage was

observed around the insert. Pictures of the vertical shear cracks and the flexure cracks are shown in Figures 4.14 and 4.15 respectively.



Figure 4.12 Insert S3-4, Plan View [Failure Mode D] **Figure 4.13** Insert S3-4, Side View [Failure Mode D]



Figure 4.14 Insert S4-2, Shear failure [Mode F] **Figure 4.15** Insert S4-2, Flexural failure [Mode F]

4.2 Discussion of Experimental Results

Table 4.1 shows a summary of the testing results presenting the maximum load carried by each insert along with the failure mode observed. The failure mode is represented by a letter in the table.

Table 4.2 provides the concrete and grout unconfined compression strengths at the time of testing (two days after production), at seven days after production, and at thirty-one days after production. In total, nine cylinder specimens were cast for the concrete

and non-shrink grout. It is important to note that the concrete and grout cylinders were not very well consolidated. The evidence of this can be seen in the large variability in the cylinder data in Table 4.2.

Table 4.1 Test Results, Max. Applied Load & Failure Mode

| Insert | Maximum Load (lb.) | Failure Mode |
|--------|--------------------|--------------|
| S 1-1 | 16,148 | B |
| S 1-2 | 11,710 | C |
| S 1-3 | 12,747 | C |
| S 1-4 | 13,515 | A |
| S 2-1 | 11,486 | B |
| S 2-2 | 17,673 | A |
| S 2-3 | 13,225 | A |
| S 2-4 | 13,404 | C |
| S 3-1 | 12,406 | C |
| S 3-2 | 12,346 | C |
| S 3-3 | 13,451 | A |
| S 3-4 | 9,560 | D |
| S 4-1 | 15,075 | C |
| S 4-2 | 16,787 | F |
| S 4-3 | 15,694 | B |
| S 4-4 | NOT TESTED | E |

Table 4.2 Concrete and Grout Strengths

| | Cyl. 1 | Cyl. 2 | Cyl. 3 | Avg. (psi) | |
|----------|--------|--------|--------|------------|--------|
| Concrete | 2,527 | 3,836 | 4,282 | 3,548 | 2 Day |
| Grout | 2,992 | 2,917 | 2,898 | 2,936 | |
| Concrete | 5,738 | 3,900 | 3,960 | 4,533 | 7 Day |
| Grout | 3,429 | 3,047 | 3,015 | 3,164 | |
| Concrete | 5,207 | 5,119 | 6,506 | 5,611 | 31 Day |
| Grout | 3,308 | 3,314 | 3,463 | 3,362 | |

Prior to discussing the results of the testing, the removal of two inserts (S3-4 and S4-4) with failures modes D & E should be noted. These inserts were damaged prior to testing as a result of testing of adjacent inserts, and therefore, the capacity obtained when testing insert S3-4 is not applicable. In addition, failure type F (Insert S4-2) unfortunately

was a plank shear failure which eventually led to plank flexural failure. This insert and the concrete around it was still in good condition when the test was stopped, therefore this was not an insert failure and is something that will have to be taken into consideration within the plank design. For the purposes of this research, this result will also be ignored as insert failures were the objective of the study. The thirteen other inserts that were tested are significant. Failure modes A, B and C are significant due to the fact that all of the inserts were intact at the beginning of the test and failure involved a shear cone similar the assumptions made both by the Dayton-Superior Product Handbook and by the PCI when treating the insert as a headed anchor stud.

A simple approach was considered to analyze the experimental data. A simple average of all thirteen capacities gives us a mean insert failure capacity of 13.76 kips, and a standard deviation of 1.85 kips. To obtain a safe maximum design capacity with 95% confidence we can take the average insert failure capacity and subtract two standard deviations to give us a capacity of 10.1 kips. If we separate the results per significant failure modes and analyze each mode individually we get the results given in Table 4.3.

If we look at the results more closely by failure mode, several observations can be made. For failure mode A, three out of the four results are in the neighborhood of thirteen kips, but the average is being influenced heavily by the 17.7 kip test data point. In a similar fashion, the average for mode B is being heavily influenced by the one low entry of 11.5 kips. Mode C has a greater number of data points (relatively speaking) and, as a result, a much smaller standard deviation. All of the data points seem to be fairly close together so an average of thirteen kips seems appropriate and no big adjustment seems necessary.

Table 4.3 Test Results, Max. Applied Load & Failure Mode

| Insert | Maximum Load (lb.) | Failure Mode | Avg. Load (lb.) | Std. Dev. (lb.) | Avg. – Std. Dev. (lb.) | Avg. – 2*(Std. Dev.) (lb.) |
|--------|--------------------|--------------|-----------------|-----------------|------------------------|----------------------------|
| S 1-4 | 13,515 | A | 14,466 | 2,142 | 12,324 | 10,182 |
| S 2-2 | 17,673 | | | | | |
| S 2-3 | 13,225 | | | | | |
| S 3-3 | 13,451 | | | | | |
| | | | | | | |
| S 1-1 | 16,148 | B | 14,442 | 2,571 | 11,871 | 9,300 |
| S 2-1 | 11,486 | | | | | |
| S 4-3 | 15,694 | | | | | |
| | | | | | | |
| S 1-2 | 11,710 | C | 13,068 | 1,278 | 11,790 | 10,512 |
| S 1-3 | 12,747 | | | | | |
| S 2-4 | 13,404 | | | | | |
| S 3-1 | 12,406 | | | | | |
| S 3-2 | 12,346 | | | | | |
| S 4-1 | 15,075 | | | | | |

If we look at the results more closely by failure mode, several observations can be made. For failure mode A, three out of the four results are in the neighborhood of thirteen kips, but the average is being influenced heavily by the 17.7 kip test data point. In a similar fashion, the average for mode B is being heavily influenced by the one low entry of 11.5 kips. Mode C has a greater number of data points (relatively speaking) and, as a result, a much smaller standard deviation. All of the data points seem to be fairly close together so an average of thirteen kips seems appropriate and no big adjustment seems necessary.

4.3 Reliability-Based Evaluation of Predictive Equation

In this section, a reliability-based evaluation of the predictive equation will be performed to begin to obtain a better understanding of the relationship between the predictive

equation and the results obtained during testing. This evaluation will form the basis of a future LRFD procedure to be developed once additional testing is done, and a clearer picture is created between the predictive equation and all of the failure modes seen during testing.

It is important to note, the average grout compressive strength on the day of testing found in Table 4.2 is 2,936 psi, and the concrete compressive strength on testing day is approximately 3,500 psi. The controlling component is the grout and its capacity along with the capacity of the system will be taken as 3,000 psi. Interestingly, the grout compressive strength does not increase significantly from the time of testing to the 31st day strength test; therefore the capacity of the system should remain fairly close to the capacities presented in this effort. In Chapter 2, calculations were run for failure cone angles ranging from sixty degrees to thirty degrees in five degree increments. All of these calculations were run using a concrete strength of 3,000 psi, therefore none of these calculations need to be altered.

The average measured capacity from the tests was 13.76 kips. Comparing this value to the predicted values with failure cones at thirty degrees and at thirty-five degrees, the calculated capacities of 12.28 kips and 12.33 kips respectively are very close to this average capacity, in fact, both of these calculated values are within one standard deviation of the average measured value.

It is very useful to evaluate the capability and reliability of the equations used to predict the insert capacity. We can define a bias factor as the insert capacity predicted divided by the experimental capacity measured. This is given by,

$$B = P_{c1}/P_{exp} \quad (4.1)$$

where: P_{c1} is the capacity predicted using equation (2.3); and P_{exp} is the experimental insert capacity measured during testing. Table 4.4 illustrates the bias factors, their mean, and their coefficients of variation for various angles and failure modes.

If we look at the mean and coefficient of variation (COV) in this ratio, the mean closest to one with the lowest coefficient of variation would suggest the most accurate prediction of strength. The bias factors (P_{c1}/P_{exp}) range from 0.861 to 0.996 when angles from 30-35 degrees are used. Angles greater than 35 degrees need not be used as the accuracy decreases as the angle increases. The coefficients of variation with 30-35 degrees are also relatively low with failure mode C predictions having the least variability. The 35 degree angle does the best overall job at predicting insert strengths for all three failure modes and does the best job at predicting the strength of failure mode C having a mean ratio of 0.959 and a COV of 0.085.

The predictive equations assume a failure shear cone with regular conic dimensions. Failure mode C follows this model quite well, but failure modes A & B seen in the experiments do not follow this assumption as closely. Evidence of this can be seen in the bias factor and COV calculations. Failure mode C at an angle of 35 degrees contains a bias factor of nearly 1.0 and the COV near zero. The other two failure modes have fairly good bias factors and a low COV but they are not as accurate as the results when failure mode C is seen in the test.

The data in Table 4.4 suggests that a 35 degree angle be used for all calculations and a bias factor of 0.865 and the COV of 0.129 can conservatively be used for modeling variability in the prediction. However, the results also suggest that predictive equations

may need to be created to model failure modes A & B. Simple adjustments to the equation for mode C may also be appropriate.

Table 4.4 Predictive Equation Results & Comparison with Experimental Results

| | | | 30 Degrees | | 35 Degrees | | 40 Degrees | | 45 Degrees | |
|--------------|----------|---------------------------|--------------------------------------|--------|--------------------------------------|--------|--------------------------------------|--------|--------------------------------------|--------|
| | | | A _o (in ²) | 80.09 | A _o (in ²) | 80.43 | A _o (in ²) | 73.95 | A _o (in ²) | 69.3 |
| | | | P _{c1} (lbs) | 12,283 | P _{c1} (lbs) | 12,334 | P _{c1} (lbs) | 11,341 | P _{c1} (lbs) | 10,628 |
| Failure Mode | Specimen | P _{exp} (lbs) | P _{c1} /P _{exp} | | P _{c1} /P _{exp} | | P _{c1} /P _{exp} | | P _{c1} /P _{exp} | |
| A | S1-4 | 13,515 | 0.909 | | 0.913 | | 0.839 | | 0.786 | |
| | S2-2 | 17,673 | 0.695 | | 0.698 | | 0.642 | | 0.601 | |
| | S2-3 | 13,225 | 0.929 | | 0.933 | | 0.858 | | 0.804 | |
| | S3-3 | 13,451 | 0.913 | | 0.917 | | 0.843 | | 0.790 | |
| | Mean | 14,466 | 0.861 | | 0.865 | | 0.795 | | 0.745 | |
| | COV | 0.148 | 0.129 | | | | | | | |
| B | S1-1 | 16,148 | 0.761 | | 0.764 | | 0.702 | | 0.658 | |
| | S2-1 | 11,486 | 1.069 | | 1.074 | | 0.987 | | 0.925 | |
| | S4-3 | 15,694 | 0.783 | | 0.786 | | 0.723 | | 0.677 | |
| | Mean | 14,442 | 0.871 | | 0.875 | | 0.804 | | 0.754 | |
| | COV | 0.178 | 0.198 | | | | | | | |
| C | S1-2 | 11,710 | 1.049 | | 1.053 | | 0.968 | | 0.908 | |
| | S1-3 | 12,747 | 0.964 | | 0.968 | | 0.890 | | 0.834 | |
| | S2-4 | 13,404 | 0.916 | | 0.920 | | 0.846 | | 0.793 | |
| | S3-1 | 12,406 | 0.990 | | 0.994 | | 0.914 | | 0.857 | |
| | S3-2 | 12,346 | 0.995 | | 0.999 | | 0.919 | | 0.861 | |
| | S4-1 | 15,075 | 0.815 | | 0.818 | | 0.752 | | 0.705 | |
| | Mean | 13,068 | 0.955 | | 0.959 | | 0.882 | | 0.826 | |
| | COV | 0.091 | 0.085 | | | | | | | |

The data in Table 4.4 forms the basis of a load and resistance factor (LRFD) approach for designing the headed anchors used in this study. However, the limited numbers of tests conducted and the resulting inability to confidently define the statistical model describing the variability/uncertainty in the predictive equation's accuracy suggests that more testing is needed before pursuing LRFD-type design methods. As a result, traditional (historic) factor of safety methods are explored.

4.4 Factor of Safety Formulation

A second approach for making a reasonable recommendation for the insert capacity is to formulate a factor of safety. A classical rule of thumb safety factor approach will be used to develop a recommended safety factor that may be used for design. The technique presented in this chapter is developed from the process presented in *The Mechanical Design Process* (Ullman 1997).

This approach presented uses contributions from five different measures when developing the factor of safety. Each measure has several parameters or rules spelled out and a factor of safety has been attached to each. To develop the safety factor, a parameter is selected from each measure and then all of the factors are multiplied together to obtain the safety factor for the system in question.

The first factor to be estimated is the contribution by the materials in the system. If the material properties of the system are well known through experiments and are known to be identical to those of the component being designed, then the factor of safety (FS_{material}) is equal to 1. If the material properties are not well known, then the FS_{material} ranges from 1.2 to 1.4.

The second factor to be estimated is the contribution for the loading demand. If the loads applied to the system are well defined as static loads, or fluctuating loads with no anticipated overloads, then the factor of safety (FS_{demand}) ranges from 1 to 1.1. If the load is expected to have potential overloads of 20 to 50 percent, then the FS_{demand} ranges from 1.2 to 1.3. And finally if the load range is not well known, then the FS_{demand} ranges from 1.4 to 1.7.

The third factor is the contribution for geometry (FS_{geometry}). If the manufacturing tolerances are closely held, then the factor of safety equals 1, but if manufacturing tolerances tend to be more relaxed, a range from 1.1 to 1.2 has been suggested.

The fourth factor is the contribution for failure limit state (FS_{limit}). If the failure limit state is derived from a uniaxial or multiaxial static stress or load, then the safety factor ranges from 1 to 1.2. If the failure limit state is not well developed and caused by cumulative damage or fatigue stresses, then a range from 1.3 to 1.5 has been suggested.

The final factor is the contribution for reliability of prediction. If the prediction reliability needs to be greater than 90 percent, then the factor of safety ($FS_{\text{reliability}}$) equals 1.1. If the prediction reliability needs to exceed 92 percent then it has been suggested that this factor range be taken as 1.2 to 1.3. Finally, if the reliability needs to exceed 99 percent, then a factor of safety range from 1.4 to 1.6 is recommended.

Applying this technique to the scenario considered in the present study, the material properties for the insert and plank are well known, therefore, $FS_{\text{material}} = 1.0$. Since the insert is being used to erect the precast plank, a possible overload due to lifting the plank, wind, suction or any other possible factors is to be expected, therefore $FS_{\text{demand}} = 1.2$. The tolerances during the manufacturing and installation process for this insert are relatively tight since the work will be done at a PCI rated plant therefore $FS_{\text{geometry}} = 1.0$. The load applied to this insert is a multi-axial temporary static load so the factor of safety for the failure theory could be argued to be 1.1, but since the expected failure is concrete controlled therefore a brittle failure, a higher factor of safety should be selected. We will take $FS_{\text{limit}} = 1.3$. Finally, the reliability in capacity prediction of the insert is high since

it will be required to lift precast plank during the erection process, therefore $FS_{\text{reliability}} =$

1.4. Combining all of these factors together a suggested factor of safety is:

$$FS = 1.0 * 1.2 * 1.0 * 1.3 * 1.4 = 2.2$$

The data in Table 4.3 suggests the following capacity of the insert using the factor of safety derived. Using all three failure modes, the average experimental load magnitude seen is 13.76 kips with a standard deviation of 1.85. Using the factor of safety derived gives:

$$P_{\text{allow}} = 13,760 \text{ lbs} / 2.2 = 6,250 \text{ lbs}$$

4.5 Recommendation

The experimental testing conducted supports two approaches for insert design. The first is a reliability-based method using predictive equations based on PCI (1992). The second is a traditional (historical) factor of safety approach.

Using the limited amount of test data generated in the present study, the mean predicted value to experimental value ratio and coefficient of variation in this ratio depends upon the failure mode. A conservative mean bias factor and coefficient of variation for 35 degree failure angle is 0.865 and 0.129, respectively. These values can serve as the basis for a proposed LRFD procedure. More testing is needed however to complete this process.

A factor of safety approach suggests that the capacity of an insert can be taken as 6.2 kips for the configuration tested with a factor of safety of 2.2. The experimental results indicate that predictive equations in PCI (1992) are appropriate for evaluating headed studs in hollow-core plank inserted using the present procedure.

Chapter 5

Conclusions & Recommendations for Future Work

5.0 Introduction

This chapter summarizes the procedure and significant results previously presented in this report. The insert capacity recommendations and safety factors are restated, and several suggestions for future work are presented to further the research and findings presented in this effort.

5.1 Summary and Conclusions

Fifteen P-52 inserts were post-installed into the cells of four precast hollowcore planks and tested to failure in an effort to evaluate their tensile capacity and compare these results to those obtained with predictive equations. The inserts were 0.75" in diameter by five-and-a half inches long, made by Dayton-Superior. The precast hollowcore planks were made by Spancrete Inc at their Valders Wisconsin precast plant and tested in the Marquette University Engineering Material and Structural Testing Laboratory

In chapter two, a summary of previous research was presented including the manufacturer's recommendations for capacity and the Precast Concrete Institute manual design procedures when treating the insert as a headed anchor stud in solid CIP concrete. The manufacturer's recommendations produce a recommended capacity of 29,600 pounds, but this does not include any reductions due to small edge distances. The manufacturer's handbook does not include recommendations for the case considered in this research, which leads to the need to research additional methods for design.

Following common recommendations (PCI 1992), a capacity of 15,400 pounds is

computed and if more recent recommendations (PCI 2007) are used, the predicted capacity is 5,900 pounds. A procedure to develop a predictive equation for the tensile capacity of the insert was presented to address these discrepancies, and the expected insert capacity was calculated failure cone models with failure angles ranging from 30 degrees to 60 degrees.

Chapter three presented the insert installation procedure along with the testing protocol used during this effort. Pictures and descriptions of the testing equipment are presented along with a step by step procedure validating its use in the testing. It should be noted that all of the testing equipment was previously sized to accommodate several tests above and beyond the requirements of this effort; therefore the design presented in chapter three was more of an adequacy check for the equipment.

Chapter four presents the results from all of the tests performed and provides a thorough description and discussion of the six failure modes observed. It should be noted that most of the inserts failed in one of three failure modes; either by forming a pullout concrete cone or by having the plank split adjacent to the insert location. A statistical analysis of all of the relevant test data is presented in the chapter. From the statistical analysis, the recommended ultimate insert capacity is 13.75 kips. The predictive capacity at thirty-five degrees is 12.3 kips, this capacity is within one standard deviation from the mean experimental capacity. The process to develop a safety factor is presented in detail in chapter four, and the recommended safety factor is 2.2. Therefore, the recommended service insert capacity is obtained by dividing the ultimate capacity for the insert of 13.75 kips and dividing it by the safety factor resulting in a capacity of 6.2 kips.

5.2 Recommendations of Future Work

There are several sections of this effort that could be further expanded to increase the accuracy and reliability of the results and proposed capacity of the P-52 insert cast into the voids of precast hollowcore planks. First and foremost, any additional research should include additional experimental testing. This will not only provide additional data points but hopefully provide a clearer picture of the major failure modes that were observed during this testing. Another potential benefit of the additional testing would be to average the results in a less conservative manner and possibly developing predictive equations and LRFD methodologies for each limit state seen in the tests. In chapter four, the data analysis showed that after separating the results by failure mode, most of the data points were clustered. Since there are a limited number of data points and the future use of this insert is for erection purposes, a more conservative approach needed to be taken. If additional data is collected in the future, the gap between the few high points and the cluster of points may be filled in or potentially the results could show that the high points are more common than what our data shows. Either way additional data points will allow us to get a better picture of each failure mode and potentially raise the insert capacity. In addition, LRFD procedures could be developed using mean, coefficient of variation (COV) and bias factors to safely size the insert in the future.

Additionally, a procedure following more closely to the ACI recommended 5% fractile capacity of the insert could be performed which would allow 5% of the inserts to fail when recommending an ultimate capacity. This would potentially raise the insert capacity but needs to be performed when the number of data points is fairly high, and a clearer picture can be derived from all of the data. The future purpose of the insert

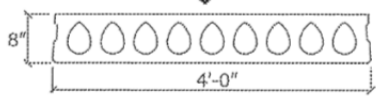
should be kept in mind when determining the higher capacity and an appropriate safety factor should be recalculated at the time to allow for any unforeseen loads that may be applied to the insert during its service life.

Finally, another section that would benefit from additional research would be to focus on the failure modes seen in the testing. The main assumption in all of the design equations presented in this effort is that the insert failure will come by the formation of a concrete pullout cone centered at the insert. Some failure modes seen suggest modified forms of the shear cone procedure. Additional research would be beneficial to determine if any alterations to the current predictive equation is needed or a second predictive equation needs to be developed to effectively predict the behavior under this failure mode.

BIBLIOGRAPHY

- Dayton (2011), *Precast Product Handbook*. Dayton Superior Corporate Headquarters. Miamisburg, OH.
- PCI (1992), *PCI Design Handbook 4th Edition*. Precast Concrete Institute. Chicago, IL.
- PCI (1999), *PCI Design Handbook 5th Edition*. Precast Concrete Institute. Chicago, IL.
- PCI (2004), *PCI Design Handbook 6th Edition*. Precast Concrete Institute. Chicago, IL.
- Shaikh and Yi (1985), “In-Place Strength of Welded Headed Studs”, *PCI Journal*, Vol. 30, No. 2, March-April
- Ullman (1997), *The Mechanical Design Process*. 2nd Ed. New York: The McGraw-Hill Companies, Inc. 314-317.

APPENDIX A

| | | | | | |
|---|--|-----------|-----------|-----------|-----------|
| 8" SPANCRETE | | | | | |
| .75" STRAND COVER | | | | | |
| NO STRUCTURAL TOPPING | | | | | |
| Dead Load Weight of Slab = 61 psf | | | | | |
| <div style="display: flex; justify-content: space-between; align-items: center;"> <div> <p>A=251 in²</p> <p>I=1817 in⁴</p> </div> <div> <p>Section Properties</p> <p>Yt=3.99 in</p> <p>Yb=4.01 in</p> </div> <div> <p>b=15.4 in</p> <p>wt= 61 psf</p> </div> </div> | | | | | |
| |  | | | | |
| eMin | 17.37 | 23 | 29.95 | 36.51 | 42.64 |
| ft-k/ft | | | | | |
| Series | .75F-8606 | .75F-8706 | .75F-8708 | .75F-8710 | .75F-8712 |
| Span in Feet | Allowable Superimposed Load In Pounds Per Square Foot | | | | |
| 13 | 468 | | | | |
| 14 | 397 | 478 | | | |
| 15 | 340 | 426 | 474 | | |
| 16 | 293 | 383 | 425 | 466 | |
| 17 | 255 | 347 | 382 | 419 | |
| 18 | 222 | 309 | 345 | 379 | |
| 19 | 195 | 273 | 316 | 345 | |
| 20 | 171 | 242 | 292 | 317 | |
| 21 | 151 | 215 | 266 | 288 | |
| 22 | 134 | 192 | 248 | 267 | 291 |
| 23 | 118 | 172 | 229 | 248 | 270 |
| 24 | 105 | 154 | 213 | 228 | 248 |
| 25 | 93 | 138 | 194 | 215 | 232 |
| 26 | 83 | 124 | 176 | 199 | 218 |
| 27 | 73 | 112 | 160 | 189 | 202 |
| 28 | 65 | 101 | 145 | 175 | 188 |
| 29 | | 91 | 132 | 164 | 177 |
| 30 | | 82 | 121 | 150 | 165 |
| 31 | | 74 | 110 | 137 | 157 |
| 32 | | | 100 | 126 | 143 |
| 33 | | | 92 | 115 | 132 |
| 34 | | | 84 | 106 | 121 |
| 35 | | | 76 | 97 | 112 |
| 36 | | | | 89 | 103 |
| 37 | | | | 82 | 95 |
| 38 | | | | 75 | 88 |
| 39 | | | | 68 | 81 |
| 40 | | | | | 74 |
| 41 | | | | | 69 |
| 42 | | | | | 63 |

Fire Rating (IBC)
 Unrestrained 0 hours
 Restrained 2 hours

CAMBER
 1"-1 1/2"
 ≥ 1 1/2"

6000 psi Concrete Strength
270 ksi Strand

6/1/2010

Appendix A Spancrete Plank Design Table

APPENDIX B

Swift Lift® System



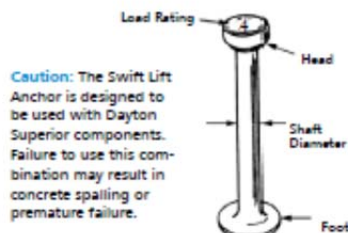
P-52 Swift Lift® Anchor

The P-52 Swift Lift Anchor is hot forged from carbon steel. The formed head provides spherical seating that the Lifting Eye engages, while a disc-shaped foot is embedded in the concrete.

Due to its being a forged part, the Swift Lift Anchor does not depend on welds or threaded engagement to develop its safe working load. Forging provides maximum safety with its advantageous material structure. This allows the anchor to easily meet the OSHA requirement of a 4 to 1 factor of safety.

In addition to the carbon steel anchors, Type 304 or 316 Stainless Steel Swift Lift Anchors are available on special order. Use stainless steel anchors when maximum protection against corrosion is required.

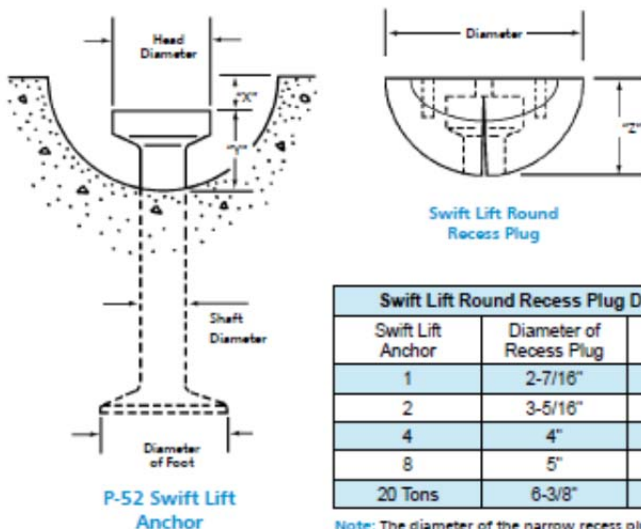
For safety, refer to the P-52 Swift Lift Anchor Selection Chart on page 31 to determine the actual safe working load of an individual anchor. The MAXIMUM safe working load is clearly visible on the head of the anchor for easy recognition of the appropriate hardware and accessories for use with each Swift Lift Anchor.



Caution: The Swift Lift Anchor is designed to be used with Dayton Superior components. Failure to use this combination may result in concrete spalling or premature failure.

To Order:
Specify: (1) quantity, (2) name,
(3) system size, (4) length
Example:
200, P-52 Swift Lift Anchors, 4 ton, 9-1/2" long

P-52 Swift Lift Anchor and Recess Plug Dimensions



| Swift Lift Round Recess Plug Dimensions | | |
|---|-------------------------|---------------|
| Swift Lift Anchor | Diameter of Recess Plug | Dimension "Z" |
| 1 | 2-7/16" | 1-3/16" |
| 2 | 3-5/16" | 1-7/16" |
| 4 | 4" | 1-13/16" |
| 8 | 5" | 2-5/16" |
| 20 Tons | 6-3/8" | 3-1/8" |

Note: The diameter of the narrow recess plug is the same as the diameter of the round recess plug.

| P-52 Swift Lift Anchor Dimensions | | | | | |
|-----------------------------------|---------------|---------------|----------------|---------------|---------------|
| Swift Lift Anchor | Dimension "X" | Dimension "Y" | Shaft Diameter | Foot Diameter | Head Diameter |
| 1 | 5/16" | 7/8" | 3/8" | 1" | 11/16" |
| 2 | 7/16" | 1-1/16" | 9/16" | 1-3/8" | 1-1/32" |
| 4 | 9/16" | 1-5/16" | 3/4" | 1-7/8" | 1-11/32" |
| 8 | 9/16" | 1-5/8" | 1-3/32" | 2-5/8" | 1-7/8" |
| 20 Tons | 9/16" | 2-5/8" | 1-1/2" | 3-3/4" | 2-3/4" |

APPENDIX C

Swift Lift® System



P-52 Swift Lift® Anchor Tensile and Shear Capacity

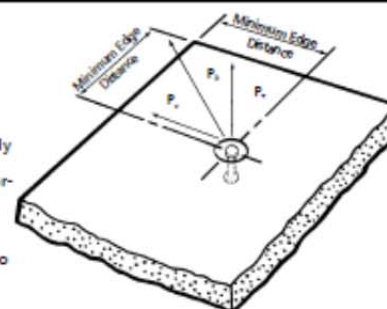
When anchors are used in the face of thin concrete elements

The following table lists the P-52 Swift Lift Anchors that are currently manufactured. Other sizes and lengths are available on special order. However, the sizes and lengths of anchors shown will handle the majority of flat precast concrete elements.

When the P-52 Swift Lift Anchor is properly embedded in normal weight concrete, the tabulated working loads are applicable for any direction of load. This applies even if the direction of load is parallel to the axis of the anchor, perpendicular to it or at any other angle.

Minimum distance between anchors is twice the minimum edge distance.

It is critical to remember that in order to obtain the safe working loads listed in the table below, the normal weight concrete must have obtained the minimum concrete strength shown, prior to initial load application.



| Swift Lift Anchor Ton x Length | Safe Working Load | Minimum Concrete Strength | Minimum Edge Distance |
|-----------------------------------|----------------------|------------------------------|--------------------------|
| 1 ton x 2-5/8" | 1,700 lbs. | 3,500 psi | 8" |
| 1 ton x 3-3/8" | 2,000 lbs. | 2,200 psi | 10" |
| 1 ton x 4-3/8" | 2,000 lbs. | 1,600 psi | 10" |
| 1 ton x 8" | 2,000 lbs. | 1,600 psi | 10" |
| 1 ton x 9-1/2" | 2,000 lbs. | 1,600 psi | 10" |
| 2 ton x 2-3/4" | 2,100 lbs. | 3,500 psi | 8" |
| 2 ton x 3-3/8" | 2,900 lbs. | 3,500 psi | 10" |
| 2 ton x 5-1/2" | 4,000 lbs. | 1,600 psi | 13" |
| 2 ton x 6" | 4,000 lbs. | 1,600 psi | 13" |
| 2 ton x 6-3/4" | 4,000 lbs. | 1,600 psi | 13" |
| 2 ton x 11" | 4,000 lbs. | 1,600 psi | 14" |
| 4 ton x 3-3/4" | 4,000 lbs. | 3,500 psi | 12" |
| 4 ton x 4-1/4" | 4,900 lbs. | 3,500 psi | 13" |
| 4 ton x 4-3/4" | 5,800 lbs. | 3,500 psi | 14" |
| 4 ton x 5-1/2" | 7,400 lbs. | 3,500 psi | 17" |
| 4 ton x 5-3/4" | 7,900 lbs. | 3,500 psi | 17" |
| 4 ton x 7-1/8" | 8,000 lbs. | 1,800 psi | 20" |
| 4 ton x 9-1/2" | 8,000 lbs. | 1,600 psi | 17" |
| 4 ton x 14" | 8,000 lbs. | 1,600 psi | 18" |
| 4 ton x 19" | 8,000 lbs. | 1,600 psi | 20" |
| 8 ton x 4-3/4" | 6,400 lbs. | 3,500 psi | 16" |
| 8 ton x 6-3/4" | 11,200 lbs. | 3,500 psi | 21" |
| 8 ton x 10" | 16,000 lbs. | 3,500 psi | 19" |
| 8 ton x 13-3/8" | 16,000 lbs. | 1,600 psi | 23" |
| 8 ton x 26-3/4" | 16,000 lbs. | 1,600 psi | 27" |
| 20 ton x 10" | 25,000 lbs. | 3,500 psi | 24" |
| 20 ton x 19-3/4" | 40,000 lbs. | 3,500 psi | 31" |

Safe Working Loads provide a factor of safety of approximately 4 to 1 in normal weight concrete. Safe Working Load is based on anchor setback from face of concrete "X" dimension, as shown on page 26.